

# Title

## Single-dose AAV-based vaccine induces a high level of neutralizing antibodies and provides long-term protection against SARS-CoV-2 in rhesus macaques

### Authors

Dali Tong<sup>1#</sup>, Mei Zhang<sup>1,2#</sup>, Yunru Yang<sup>1,2#</sup>, Han Xia<sup>3,4#</sup>, Haiyang Tong<sup>5</sup>, Weihong Zeng<sup>2</sup>, Muziying Liu<sup>6</sup>, Huan Ma<sup>2</sup>, Xue Hu<sup>3</sup>, Weiyong Liu<sup>1</sup>, Yuan Cai<sup>1</sup>, Yanfeng Yao<sup>4</sup>, Yichuan Yao<sup>1,2</sup>, Kunpeng Liu<sup>3</sup>, Shifang Shan<sup>7</sup>, Yajuan Li<sup>8</sup>, Ge Gao<sup>4</sup>, Weiwei Guo<sup>3</sup>, Yun Peng<sup>4</sup>, Shaohong Chen<sup>3</sup>, Juhong Rao<sup>3</sup>, Jiaxuan Zhao<sup>3</sup>, Juan Min<sup>4</sup>, Qingjun Zhu<sup>5</sup>, Yanmin Zheng<sup>5</sup>, Lianxin Liu<sup>1</sup>, Chao Shan<sup>3</sup>, Kai Zhong<sup>5</sup>, Zilong Qiu<sup>7\*</sup>, Tengchuan Jin<sup>1,2\*</sup>, Zhiming Yuan<sup>4\*</sup>, Tian Xue<sup>1,2,7,9\*</sup>†

### Affiliations:

<sup>1</sup>First Affiliated Hospital of USTC, School of Life Sciences, Division of Life Sciences and Medicine, University of Science and Technology of China, Hefei 230026, China

<sup>2</sup>Hefei National Laboratory for Physical Sciences at the Microscale, Neurodegenerative Disorder Research Center, CAS Key Laboratory of Brain Function and Disease, CAS Key Laboratory of Innate Immunity and Chronic Disease, University of Science and Technology of China, Hefei 230026, China

<sup>3</sup>State Key Laboratory of Virology, Wuhan Institute of Virology, Chinese Academy of Sciences, Wuhan 430071, China

<sup>4</sup>Center for Biosafety Mega-Science, Wuhan Institute of Virology, Chinese Academy of Sciences, Wuhan 430071, China

<sup>5</sup>Hefei Institutes of Physical Science, Chinese Academy of Sciences, Hefei 230031, China

<sup>6</sup>Anhui Institute of Pediatric Research, Anhui Provincial Children's Hospital, Hefei 230051, China

<sup>7</sup>Chinese Academy of Sciences Center for Excellence in Brain Science and Intelligence Technology, Chinese Academy of Sciences, Shanghai 200031, China

<sup>8</sup>Department of Clinical Laboratory, the First Affiliated Hospital of Anhui Medical University, Hefei, 230022, China

<sup>9</sup>Institute for Stem Cell and Regeneration, Chinese Academy of Sciences, Beijing 100101, China

<sup>#</sup>These authors contributed equally

<sup>\*</sup>Corresponding authors:

Tian Xue, [xuetian@ustc.edu.cn](mailto:xuetian@ustc.edu.cn) (†lead contact)

Zhiming Yuan, [yzm@wh.iov.cn](mailto:yzm@wh.iov.cn)

Tengchuan Jin, [jint@ustc.edu.cn](mailto:jint@ustc.edu.cn)

Zilong Qiu, [zqiu@ion.ac.cn](mailto:zqiu@ion.ac.cn)

## Abstract

Coronavirus disease 2019 (COVID-19), which is triggered by severe acute respiratory syndrome coronavirus 2 (SARS-CoV-2) infection, continues to threaten global public health. Developing a vaccine that only requires single immunization but provides long-term protection for the prevention and control of COVID-19 is important. Here, we developed an adeno-associated virus (AAV)-based vaccine expressing a stable receptor-binding domain (SRBD) protein. The vaccine requires only single shot, but provides effective neutralizing antibodies (NAbs) over 300 days in rhesus macaques (*Macaca mulatta*). In addition, the NAbs are at much higher levels than seen in the sera of convalescent patients. It is worth to note that though we detected the pre-existing AAV2/9 NAbs before immunization, the vaccine still induced high and effective NAbs, and did not boost the AAV2/9 NAbs levels in rhesus macaques. Importantly, AAV-SRBD immune sera efficiently neutralized the SARS-CoV-2 P.1/P.2, B.1.1.7, and B.1.351 variants. Together, all the data suggest the vaccine has great potential in preventing the spread of SARS-CoV-2.

**Key words:** COVID-19 vaccine, AAV, SARS-CoV-2, single dose, long-term protection

## Main

Coronavirus disease 2019 (COVID-19) is a highly infectious respiratory disease and continues to pose a serious global public health emergency. On 18 May 2021, the World Health Organization (WHO) reported over 163 million confirmed cases and 3.3 million deaths globally. The disease shows a high infection rate, long incubation period, and rapidly emerging variants, which have led to its rapid spread worldwide<sup>1</sup>. Many vaccines have been developed to varying stages for the control of severe acute respiratory syndrome coronavirus 2 (SARS-CoV-2), the virus responsible for COVID-19, including vaccines based on messenger RNA (mRNA)<sup>2,3</sup>, DNA<sup>4</sup>, viral vectors<sup>5,6</sup>, inactivated SARS-CoV-2<sup>7,8,9</sup>, and recombinant proteins<sup>10</sup>. Indeed, several vaccines have been approved by the United States Food and Drug Administration (FDA), which have been shown to effectively protect patients from SARS-CoV-2 infection. However, these vaccines lack long-term antibody protection data, and most require multiple injections to induce stable neutralizing antibodies (NAbs). Therefore, developing a vaccine that only requires single-dose immunization but provides long-term protection for the prevention and control of COVID-19 would be optimal.

Adeno-associated virus (AAV) is a single-stranded DNA parvovirus widely used for gene therapy<sup>11,12</sup>. AAV vectors have special features that are highly beneficial for clinical applications. For instance, AAVs have low immunogenicity and rarely cause immune inflammation; AAVs can stably express foreign genes over a long period and are easy to produce; and AAVs belong to the safest Risk Group 1 (RG1) level of biotechnology products and are considered safe gene delivery vectors. Several AAV vector-mediated gene therapy products have been approved by the FDA for the treatment of inherited blindness, spinal muscular atrophy, and Duchenne muscular dystrophy<sup>13</sup>. Thus, we applied AAV vectors in the current study to develop a long-term expression vaccine for the prevention of COVID-19. The AAV2/9 serotype was chosen as the vaccine carrier due to its high transduction efficiency in muscles<sup>14</sup>.

The SARS-CoV-2 spike protein mediates the binding of the virus to the human

angiotensin converting enzyme 2 (ACE2) receptor for entry into target cells<sup>15</sup>. As such, it is the main antigen target for vaccines. Based on the SARS-CoV-2 spike protein structure (PDB: 6VXX), we found that the receptor-binding domain (RBD) was not stable. Therefore, to stabilize the antigen, we designed a stable receptor-binding domain (SRBD) that spanned the spike protein from Q321 to S591 with a C and N tail to form a beta-sheet (Figure 1 a and b). For comparison, we designed two other vaccines, named S12 and S2. The S12 vaccine contained the signaling sequence (SS), N-terminal domain (NTD), RBD, and SD1, SD2, and S1/S2 subdomains of the spike protein driven by the cytomegalovirus early enhancer chicken/ $\beta$ -actin (CAG) promoter. The S2 vaccine contained all amino acids in S12 plus the S2' domain (Figure S1a). Thermal stability analysis proved that the SRBD protein was more thermostable than RBD alone (Figure 1c).

To assess the immunogenicity of these AAV vaccines, we injected four types of vaccines (i.e., S12, S2, RBD, and SRBD) intramuscularly into C57BL/6J mice at a dose of  $1 \times 10^{11}$  virus genomes (vg)/mouse (Figure S1b). AAV-CAG-GFP ( $1 \times 10^{11}$  vg/mouse) was used as a control. Blood samples from the C57BL/6J mice were collected on days 14, 21, 28, 35 and 42 post injection. Compared with the control, NAbs were only detected in the AAV-CAG-SRBD mouse group (Figure 1d), thus we chose SRBD as the antigen target for further study. In addition, SRBD was detected in the injected left leg muscle (injected muscle, IM) but not in the right leg muscle (opposite muscle, OM; Figure S1c). Histological analysis illustrated that no significant pathological changes occurred in the major tissues of AAV-injected mice, e.g., lung, heart, liver, spleen, and kidney, compared with the control group (Figure 1e). These results suggest that the SRBD vaccine exhibited good immunogenicity and safety in mice.

For further examine vaccine safety and efficiency, we evaluated the immunogenicity and protective efficacy of the SRBD vaccine in a nonhuman primate (NHP) species. Specifically, 13 rhesus macaques (*Macaca mulatta*) were randomly divided into three groups and received a single-dose immunization of  $1 \times 10^{12}$

vg/macaque (high-dose, seven macaques),  $1 \times 10^{11}$  vg/macaque (middle-dose, three macaques), or  $1 \times 10^{10}$  vg/macaque (low-dose, three macaques) of SRBD, respectively. AAV-CAG-GFP/macaque ( $1 \times 10^{12}$  vg) was used as the control vaccine (three macaques). All intramuscular-injected macaques showed normal body weight post injection (Figure S2a). Blood samples from the macaques were collected for testing NAb (Figure 2a). One potential limitation of AAV vaccine application is that most humans and macaques have experienced wild-type AAV exposure, which can result in pre-existing AAV NAb and inhibition of AAV transduction in primates<sup>16</sup>. Given this, we tested the levels of AAV NAb in the macaques before and after vaccination. First, we randomly selected seven macaques (two macaques each in the low- and middle-dose groups and three macaques in the high-dose group) to test their pre-existing levels of AAV NAb. All tested macaques were found to be NAb-positive, suggesting that AAV2/9 NAb may commonly pre-exist in this species (Figure 2b). Furthermore, the AAV NAb levels did not change significantly from days 0 to 56 in the different groups. Even in the long-term high-dose macaques, AAV NAb remained at a similar level from days 0 and 217. These results suggest the existence of AAV NAb in macaques before immunization, and that intramuscular injection of the AAV vaccine did not boost AAV NAb levels.

Even though AAV NAb pre-existed in the macaque blood samples, the levels of SRBD NAb in all macaques were determined at different days post injection (Figure 2c-e). The SRBD vaccine demonstrated good immunogenicity in the high- and middle-dose macaques, but not in the low-dose macaques (Figure 2c, Figure S2c-d). In addition, the seroconversion rate (antibody titer  $> 1 \times 1000$ ) reached 100% on day 35 after immunization in the high- (7/7) and middle-dose (3/3) macaques, but only 33.3% on day 56 in the low-dose macaques (1/3). These results suggest that the pre-existing AAV NAb did not prevent the transduction of the AAV vaccine in the muscle cells following intramuscular injection. We also monitored the NAb levels in the high-dose macaques from days 0 to 308. Results indicated that NAb emerged on day 21 in the high-dose group and remained at a high level until day 308, with a much higher titer

than found in the mixed sera of convalescent patients (H-M) (Figure 2d-e)<sup>17, 18</sup>. Competitive enzyme-linked immunosorbent assay (ELISA) showed that at day 42, the NAbs in the high-dose macaques effectively inhibited the interaction between the RBD and ACE2, and the efficacy was better than that in H-M sera (Figure 2f-g). The inhibition ability of the NAbs was maintained from days 70 (Figure S2e-f) to 308 post injection (Figure 2f-g). The pre-existing AAV NAbs and stably expressed SRBD NAbs detected in the macaques suggest that AAV NAbs do not inhibit the immunity of AAV-delivered vaccines. We next tested the protection ability of NAbs against real SARS-CoV-2 (2019-nCoV-WIV04) in Vero E6 cells using plaque reduction neutralization test (Figure 2h-j). Notably, sera from the high-dose group at days 42 and 126 post injection effectively protected the Vero E6 cells from SARS-CoV-2 infection. In particular, the 50% plaque-reduction neutralization test (PRNT50) of serum in the high-dose macaques on day 126 reached  $10^4$ , indicating that the vaccine has a high protection ability (Figure 2j). The above results suggest that the SRBD vaccine induced high and effective NAbs in rhesus macaques despite the pre-existence of AAV NAbs in their blood before immunization.

The long-term toxicity of the SRBD vaccine was further evaluated in the rhesus macaques. As of day 308, no deaths, impending deaths, or significant abnormalities in clinical physiology were found in any macaque. Widely analyzed pathological indicators also showed that lymphocyte subgroup ( $CD20^+$ ,  $CD3^+$ ,  $CD3^+CD4^+$ , and  $CD3^+CD8^+$ ) distribution was normal before and after intramuscular injection (Figure 3a-d). In addition, T helper 1 cells (Th1) labeled with IFN- $\gamma$  and TNF- $\alpha$  and T helper 2 cells (Th2) labeled with IL-10 were unchanged before and after injection (Figures 3e, 3f, and 3i). The IFN- $\gamma$ -, TNF- $\alpha$ -, and IL-10-positive  $CD8^+$  T cells were found at a similar proportion before and after vaccination (Figure 3g, 3h, and 3j). Other pathological indicators of blood, i.e., white blood cell (WBC), monocyte (MONO), neutrophil (NEUT), eosinophil (EO), basophil (BASO), lymphocyte (LYMPH), red blood cell (RBC), and platelet (PLT) counts, were also normal before and after immunization with different doses of the AAV vaccine (Figure S3). These results

suggest that the vaccine did not induce T cell-specific responses after vaccination.

To evaluate the safety of the AAV SRBD vaccine, the expression of SRBD was analyzed in the livers of the macaques (Figure S4a). The mRNA expression of SRBD was detected in the high-dose macaques but not in middle-dose group. As it is technically difficult to analyze the AAV-based gene expression in all major organs of macaques, the expression of GFP was analyzed in the major organs of mice (Figure S4b-c). Results showed that GFP signaling was found in the injected muscle cells and liver cells of mice, but not in other major organs, i.e., heart, lung, spleen, or kidney, even in the high-dose group. Hepatic function tests indicated that there was no liver function damage in the macaques after AAV injection (Figure S5a-d). Thus, the AAV vector was deemed to be safe, even at the highest dose tested ( $1 \times 10^{12}$  vg/ macaque).

Recently, SARS-CoV-2 variants P.1/P.2, B.1.1.7, and B.1.351 have spread rapidly worldwide<sup>19, 20</sup>. Of concern, certain approved vaccines have shown lower protective efficiency against these variants. To test the protection ability of the SRBD NAb to different SARS-CoV-2 variants, we generated several RBD mutant proteins (P.1/P.2 with K417T, E484K, and N501Y; B.1.1.7 with N501Y and A570D; and B.1.351 with K417N, E484K, and N501Y). Competitive ELISA showed that the macaque serum effectively inhibited the interactions between the RBD mutants (P.1/P.2, B.1.1.7, and B.1.351) and ACE2 (Figure 4a-d). Therefore, the SRBD NAb appear to offer long-term protection against SARS-CoV-2 variant RBDs (Figure 4e-j). As the N501Y mutation is found in all three SARS-CoV-2 variants, we evaluated the interactions between the RBD N501Y mutant and SRBD NAb. Results indicated that the SRBD NAb from the middle- and high-dose macaques interacted with the RBD N501Y mutant and inhibited interactions between the RBD N501Y mutant and ACE2 (Figure S6). Thus, these results indicate that the SRBD vaccine has the potential to block infection from SARS-CoV-2 variants.

In conclusion, we developed a single-dose vaccine that can provide long-term protection against SARS-CoV-2. Our results show that SRBD is not only more



thermostable than RBD alone but can also trigger high NAb production. The vaccine can maintain SRBD NAb for more than 300 days, providing high levels of NAb and long-term protection without damaging the main tissues of the tested macaques. Importantly, the pre-existing AAV NAb in primates did not impact the effectiveness of the AAV-based vaccine, on the other hand, the injection of AAV-based vaccine does not boost AAV NAb. Therefore, it may be possible for patients to receive multiple AAV-based vaccinations. More importantly, the SRBD vaccine provides protective effects against emerging variants. Therefore, this vaccine highlights a new avenue for the control of SARS-CoV-2.

## Materials and Methods

### Animal husbandry samples

C57BL/6 Mice and rhesus macaques (*Macaca mulatta*) were maintained at 25 °C on a 12 h: 12 h light:dark cycle in an animal room at the University of Science and Technology of China. All procedures were conducted in accordance with the Principles for the Ethical Treatment of Animals approved by the Animal Care and Use Committee at the University of Science and Technology of China (202006220919000464981). The macaques received a single-dose immunization (1 mL) of  $1 \times 10^{12}$  vg/macaque (high-dose),  $1 \times 10^{11}$  vg/macaque (middle-dose),  $1 \times 10^{10}$  vg/macaque (low-dose) of SRBD, and  $1 \times 10^{12}$  vg/macaque of AAV-CAG-GFP as control by intramuscular injection. Mice received a single-dose immunization (20  $\mu$ L) of  $1 \times 10^{11}$  vg/mouse of SRBD, RBD, S1, S2 or AAV-CAG-GFP. For the immunohistochemistry analysis, mice received different doses ( $1 \times 10^{11/10/9}$  vg/mouse) of AAV-CAG-GFP.

### AAV-package

The AAV vaccines were packaged in HEK-293T cells. In brief, 10  $\mu$ g of pHelper vector, 5  $\mu$ g of AAV2/9 vector, and 5  $\mu$ g of pITR vector (S2/S12/RBD/SRBD/GFP) were transfected into a 10-cm diameter dish with HEK-293T cells by

Polyethylenimine (PEI) (PolyScience, Niles, USA). The HEK-293T cells were cultured with Dulbecco's Modified Eagle Medium (DMEM, Gibco, 11965-092) and 10% fetal bovine serum (Gibco, 16000-044) at 37 °C. The supernatant of HEK-293T cells was harvested at days 3 and 6 after transfection. The supernatant was concentrated with Ultra-15 Centrifugal Filters (Millipore, UFC905024) and then gradient-purified with 15% to 60% Optiprep (Sigma, D1556). The AAV vaccine was harvested and washed using phosphate-buffered saline (PBS) six times, then diluted in 150  $\mu$ L of PBS. The titers of the AAV vaccines were calculated by quantitative real-time polymerase chain reaction (qRT-PCR). The AAV vaccines were stored at -80 °C.

### **Electron microscope (EM) sample preparation**

The AAV vaccines ( $1 \times 10^{12}$  vg/mL) were added to carbon-coated copper grids previously glow-discharged at low air pressure and stained with 2% uranyl acetate for 90 s. The EM was operated at an acceleration voltage of 120 kV. Images were recorded using a Tecnai G2 Spirit 120kV electron microscope at 23,000 $\times$  magnification.

### **Protein expression and purification**

The methods for purifying the SARS-CoV-2 RBD [amino acid (AA) 321–591], SARS-CoV-2 RBD variants, and human ACE2 extracellular domain (AA 19 to 615) followed previous research<sup>18</sup>. In brief, target genes were inserted into the pTT5 vector, which contains a IFNA1 signal peptide at the N-terminus and a TEV enzyme site connected to the human IgG1 Fc at the C-terminus. The expression vectors were then transiently transfected into the HEK-293F cells using polyethyleneimine (Polyscience). After 3 days, the supernatant was collected by centrifugation at 5,000  $\times$ g for 15 min at 4°C. About ¼ volume of 1  $\times$  PBS was added to adjust the pH of the supernatant. The supernatant was then loaded onto the protein A column and the target protein was eluted with 0.1 M acetic acid on ÄKTA pure (GE Healthcare). The

collected protein was added to 1 mM Edetate disodium (EDTA), 5 mM dithiothreitol (DTT), and TEV enzyme to remove Fc on a shaker in a 4 °C freezer. After dialysis in  $1 \times$  PBS, tandem protein A and nickel columns were used for further purification. Both Fc and undigested protein were loaded onto the protein A column and TEV (6  $\times$  His tag) was loaded onto the nickel column. The target protein was collected during flow through.

### **Thermal stability analysis**

To compare the thermal stability of RBD and SRBD, circular dichroism (CD) spectra were acquired on a Chirascan Spectrometer (Applied Photophysics, Leatherhead, UK). Prior to CD measurements, the sample buffers were changed to PBS and the protein concentration was adjusted to 0.5 mg/mL, as determined by its absorbance at 280 nm. For thermal titration, CD spectra were acquired from 20 to 95 °C with temperature steps of 5 °C and wavelengths between 180–260 nm. The CD signals at 222 nm were used to characterize structural changes during thermal titration. The data were fitted by Prism v6 to calculate the  $T_m$  values.

### **Vaccine immunogenicity analysis**

The C57BL/6J mice (8 weeks old; male and female; 20–25 g body weight) were randomly divided into five groups (5 mice per group). The mice were intramuscularly injected with four kinds of AAV vaccines or the AAV-CAG-GFP control at a dose of  $1 \times 10^{11}$  vg (20  $\mu$ L). The macaques were randomly divided into four groups (7 macaques in high-dose group and 3 macaques in other groups) and intramuscularly injected with 1 mL of SRBD vaccine ( $1 \times 10^{12}/10^{11}/10^{10}$  vg for high/middle/low dose) or AAV-CAG-GFP control ( $1 \times 10^{12}$  vg). Blood was collected from macaques before immunization and every 7 days before day 42 after injection and every 14 or 21 days after day 42.

### **ELISA and competitive ELISA**

Nunc MaxiSorp plates were coated with 2 µg/mL (for ELISA) or 3 µg/mL (for competitive ELISA) recombinant RBD, RBD N501Y, P.1/P.2 RBD, B.1.1.7 RBD, or B.1.351 RBD, or 3 µg/mL AAV9 at 4 °C overnight. After washing four times with PBS (3 min each time), the plates were blocked by 5% no-fat milk in PBS at room temperature for 2 h. Serially diluted serum (5% no-fat milk in PBST (PBS with 0.1% Tween-20) for ELISA or 5% no-fat milk in PBST with 15 nM biotin-ACE2-TEV-Fc for competitive ELISA) was added to the plates, which were then incubated at room temperature for 1 h. After washing three times with PBST (3 min each time), horseradish peroxidase (HRP)-conjugated goat anti-mouse IgG (Sangon Biotech, D110087, mouse serum, ELISA), rabbit anti-monkey IgG (Cellwaylab, C020217, macaque serum, ELISA), or HRP-conjugated streptavidin (Beyotime, A0303, competitive ELISA) were added, followed by incubation at room temperature for 1 h. For macaque serum ELISA, HRP-conjugated goat anti-rabbit IgG (Sangon Biotech, D110058) was added, followed by incubation at room temperature for 1 h. After washing three times with PBST (3 min each time), TMB substrate (Beyotime, P0209) was added for 8 min, then stopped by 1 M H<sub>2</sub>SO<sub>4</sub>. Absorbance at 450 nm was measured with a microplate reader.

### **Plaque reduction neutralization test in Vero E6 cell assay**

The macaque serum samples were tested using a plaque reduction neutralization test (PRNT) for SARS-CoV-2 (2019-nCoV-WIV04) in the BSL-3 Laboratory. Briefly, serum was heat inactivated at 56 °C for 30 min and diluted to 1:50, followed by three-fold serial dilutions (1:50, 1:150, 1:450, 1:1350, 1:4050, and 1 : 12150). The serum was then mixed with 100 PFU of the virus and incubated at 37 °C for 1 h. The virus-serum dilution mixtures and virus control were then inoculated into Vero E6 cell monolayers in 24-well plates for 1 h, before adding an overlay medium including 1.5% methylcellulose at 37 °C for 4–5 days to allow plaque development. The plates were then fixed and stained with 2% crystal violet in 30% methanol for 30 min at room temperature, after which the plaques were manually counted and measured. The

PRNT titer was calculated based on a 50% reduction in plaque count (PRNT50).

## **RT-PCR**

Total RNA was extracted from organs with Trizol (Invitrogen, 15596026) and PrimeScript RT Reagent Kit (Takara, RR037A). Forward and reverse primers were designed to target SRBD (Forward: 5'-AATGGCGTGGAGGGCTTTAA-3' and Reverse: 5'-GCAAGGTGTGATGTCCAGGA-3').

## **Hematoxylin-eosin (H&E) staining**

Mice were anesthetized with sodium pentobarbital (40 mg/kg, intraperitoneal injection), then perfused with PBS and fixed in 4% paraformaldehyde (PFA). Organs were post-fixed in 4% paraformaldehyde overnight at 4 °C, then dehydrated in 15% and 30% sucrose, respectively. Organs were sectioned at a thickness of 10 µm for H&E staining with a freezing microtome. Isopropanol (500 µL) was added to the slices and incubated at room temperature for 1 min. The slices were air dried, stained with hematoxylin (Agilent, S330930-2, 1 mL), and incubated at room temperature for 7 min. The slices were then washed 10 times (10 s each time) with ultrapure water, followed by the addition of bluing buffer (Agilent, CS70230-2, 1 mL) and incubation at room temperature for 2 min. After washing five times with ultrapure water (10 s each time), eosin mix (Sigma, HT110216, 1 mL) was added, and the sections were incubated at room temperature for 1 min.

## **Immunohistochemical analysis**

Organs (muscle, liver, heart, lung, spleen, and kidney) were sectioned (40-µm thick) for immunohistochemical analysis with a freezing microtome. After washing with PBS three times (5 min each time), the slices were blocked with 3% bovine serum albumin (BSA) and 0.1% Triton-X100 in PBS for 1 h at room temperature. The slices were then stained using 1:1000 anti-GFP antibody (Earthox, E002030-02) in blocking buffer overnight at 4 °C. Slices were washed with PBS three times (15 min

each time) and incubated with secondary antibodies Alexa Fluor 488 donkey anti-mouse IgG (1: 1000, Thermo Scientific, A21202) for 2 h at room temperature. DAPI (1:1000, Thermo Scientific, D3571) was used to stain cell nuclei. Confocal images were captured using a Leica microscope.

### **Peripheral blood mononuclear cells (PBMCs), exocellular and intracellular staining, and flow cytometry**

Blood samples from macaques were collected in EDTA-2K tubes. Ficoll medium (3 mL, Solarbio, P4350) was first added into a 15-mL tube, followed by blood (3 mL) and density gradient centrifugation at 400  $\times g$  for 20 min at room temperature (ACC/DEC: 6/2). The plasma was then collected and stored at  $-80^{\circ}\text{C}$ . CELLSAVING buffer (Xinsaimei, C40100) was used to resuspend the PBMCs after thorough washing with PBS, the cells then stored at  $-80^{\circ}\text{C}$ .

The frozen cells were resuspended and washed in RPMI medium 1640 (Gibco). Anti-CD3 (BD, 557705), anti-CD4 (BioLegend, 357423), anti-CD8 (BioLegend, 301007), and anti-CD20 (BioLegend, 302310) antibodies were added to the cells for staining for 30 min in the dark on ice. After washing with PBS (30 s), the cells were tested on the BD FACSVerse flow cytometer. The PBMCs were also resuspended in RPMI medium 1640, with a cocktail (BD Biosciences, 550583) added to activate the cells at  $37^{\circ}\text{C}$  for 4 h. Cells were washed with  $1 \times$  PBS (30 s) and stained on ice in the dark for 30 min with anti-CD3 (BD, 557705), anti-CD4 (BioLegend, 357423), and anti-CD8 (BioLegend, 344714). The cells were then fixed and permeabilized using a Cytofix/Cytoperm Soln Kit (BD Biosciences, 554714). Afterwards, cells were stained with anti-IFN- $\gamma$  (BioLegend, 502526), anti-TNF- $\alpha$  (BioLegend, 502930), and anti-IL-10 (BioLegend, 501420) antibodies and incubated on ice in the dark for 1 h. After washing with PBS (30 s), the cells were tested on the BD FACSVerse flow cytometer. FlowJo v10 software was used for data analysis.

### **Statistical analyses**

All data are presented as means  $\pm$  standard error of the mean (SEM), except for the titers of NAb, which were quantified using geometric mean + geometric standard deviation. Student's *t*-test was used to determine the statistical significance of differences in Figure 1c. One-way analysis of variance (ANOVA) and two-way ANOVA were used to determine the statistical significance of the bar and curve graphs, respectively. Quantification graphs were analyzed using GraphPad Prism v6 (GraphPad Software). \*:  $p < 0.05$ ; \*\*:  $p < 0.01$ ; \*\*\*:  $p < 0.001$

## Acknowledgments

We thank all colleagues from the National Biosafety Laboratory (Wuhan), Chinese Academy of Sciences, China, for their support during the study. We thank the Center for Instrumental Analysis and Metrology and Biosafety Level 3 Laboratory, Wuhan Institute of Virology, Wuhan, China. This work was supported by Joint Laboratory of Innovation in Life Sciences University of Science and Technology of China (USTC) and Changchun Zhuoyi Biological Co. Ltd, the Strategic Priority Research Program of the Chinese Academy of Sciences (XDA16020603 and XDB39000000), the National Key Research and Development Program of China (2020YFA0112200), (81925009, 81790644, 81900855, 82000941), the Fundamental Research Funds for the Central Universities. The study was also supported by the Anhui Provincial Natural Science Foundation (1808085MH289 to M.Z.)

## Author contributions

T.X., Z.Y., T.J and Z.Q. conceived the project and designed the experiments. D.T. and M.Z. developed the vaccines, tested their immunogenicity and safety, and wrote the manuscript. Y.Y. constructed SARS-CoV-2 variants, coated the ELISA plates and performed flow cytometry. H. X. performed neutralizing antibody assay in Vero E6 cells. H.T., W. Z., M. L., H. M., X. H., W. L., Y. C., Y. Y., Y. Y., K. L., S. S., Y. L., G. G., W. G., Y. P., S. C., J. R., J. Z., J. M., Q. Z., Y. Z., L. L., C. S., K. Z. worked on data collection, analysis and discussion. All authors edited and proofread the manuscript.

## **Competing interests**

T.X., T.J., Y.C., M. Z. and D. T. are inventors on a pending patent related to this work filed by the University of Science and Technology of China (no. 202010903143.9, filed on 3 December 2020). The authors declare no other competing interests.



## References

1. Krammer, F. SARS-CoV-2 vaccines in development. *Nature* **586**, 516-527 (2020).
2. Polack, F.P. *et al.* Safety and Efficacy of the BNT162b2 mRNA Covid-19 Vaccine. *N Engl J Med* **383**, 2603-2615 (2020).
3. Baden, L.R. *et al.* Efficacy and Safety of the mRNA-1273 SARS-CoV-2 Vaccine. *N Engl J Med* **384**, 403-416 (2021).
4. Smith, T.R.F. *et al.* Immunogenicity of a DNA vaccine candidate for COVID-19. *Nat Commun* **11**, 2601 (2020).
5. Ramasamy, M.N. *et al.* Safety and immunogenicity of ChAdOx1 nCoV-19 vaccine administered in a prime-boost regimen in young and old adults (COV002): a single-blind, randomised, controlled, phase 2/3 trial. *Lancet* **396**, 1979-1993 (2021).
6. Zhu, F.C. *et al.* Immunogenicity and safety of a recombinant adenovirus type-5-vectored COVID-19 vaccine in healthy adults aged 18 years or older: a randomised, double-blind, placebo-controlled, phase 2 trial. *Lancet* **396**, 479-488 (2020).
7. Xia, S. *et al.* Safety and immunogenicity of an inactivated SARS-CoV-2 vaccine, BBIBP-CorV: a randomised, double-blind, placebo-controlled, phase 1/2 trial. *Lancet Infect Dis* **21**, 39-51 (2021).
8. Wu, Z. *et al.* Safety, tolerability, and immunogenicity of an inactivated SARS-CoV-2 vaccine (CoronaVac) in healthy adults aged 60 years and older: a randomised, double-blind, placebo-controlled, phase 1/2 clinical trial. *Lancet Infect Dis* (2021).
9. Zhang, Y. *et al.* Safety, tolerability, and immunogenicity of an inactivated SARS-CoV-2 vaccine in healthy adults aged 18-59 years: a randomised, double-blind, placebo-controlled, phase 1/2 clinical trial. *Lancet Infect Dis* **21**, 181-192 (2021).
10. Yang, J. *et al.* A vaccine targeting the RBD of the S protein of SARS-CoV-2 induces protective immunity. *Nature* **586**, 572-577 (2020).
11. Bravo-Hernandez, M. *et al.* Spinal subpial delivery of AAV9 enables widespread gene silencing and blocks motoneuron degeneration in ALS. *Nat Med* **26**, 118-130 (2020).
12. Bennett, J. *et al.* Safety and durability of effect of contralateral-eye administration of AAV2 gene therapy in patients with childhood-onset blindness caused by RPE65 mutations: a follow-on phase 1 trial. *Lancet* **388**, 661-672 (2016).
13. Wang, D., Tai, P.W.L. & Gao, G. Adeno-associated virus vector as a platform for gene therapy

delivery. *Nat Rev Drug Discov* **18**, 358-378 (2019).

14. Zincarelli, C., Soltys, S., Rengo, G. & Rabinowitz, J.E. Analysis of AAV serotypes 1-9 mediated gene expression and tropism in mice after systemic injection. *Mol Ther* **16**, 1073-1080 (2008).
15. Shang, J. *et al.* Cell entry mechanisms of SARS-CoV-2. *Proc Natl Acad Sci U S A* **117**, 11727-11734 (2020).
16. Li, C. *et al.* Neutralizing antibodies against adeno-associated virus examined prospectively in pediatric patients with hemophilia. *Gene Ther* **19**, 288-294 (2012).
17. Zeng, W. *et al.* Characterization of SARS-CoV-2-specific antibodies in COVID-19 patients reveals highly potent neutralizing IgA. *Signal Transduct Target Ther* **6**, 35 (2021).
18. Ma, H. *et al.* Potent Neutralization of SARS-CoV-2 by Hetero-bivalent Alpaca Nanobodies Targeting the Spike Receptor-Binding Domain. *J Virol* (2021).
19. Wang, P. *et al.* Antibody resistance of SARS-CoV-2 variants B.1.351 and B.1.1.7. *Nature* **593**, 130-135 (2021).
20. Hoffmann, M. *et al.* SARS-CoV-2 variants B.1.351 and P.1 escape from neutralizing antibodies. *Cell* **184**, 2384-2393 e2312 (2021).

## Figures and legends

Fig. 1

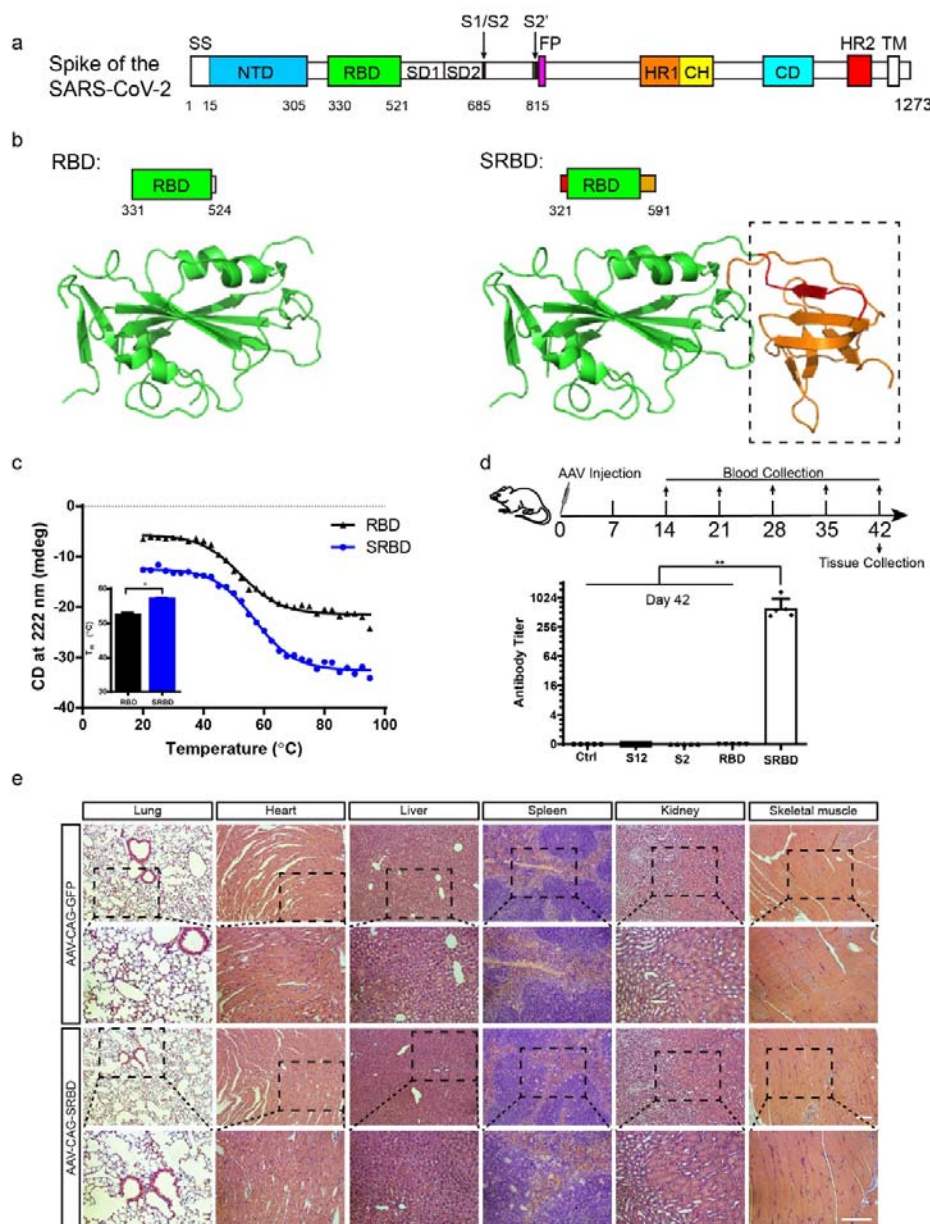


**Figure 1. Immunogenicity of AAV-delivered SARS-CoV-2 vaccines in mice.**

(a) Overall topology of the SARS-CoV-2 spike monomer. SS, signaling sequence; NTD, N-terminal domain; RBD, receptor-binding domain; SD1, subdomain 1; SD2, subdomain 2; HR1, heptad repeat 1; CH, central helix; CD, connector domain; HR2,

heptad repeat 2; TM, transmembrane domain.

(b) Structural analysis of RBD and SRBD. A stable  $\beta$ -sheet was form between Red section (Q321 to P330) and orange section (C525 to S591).

(c) Thermal stability of RBD and SRBD proteins by CD spectrum. The thermal denaturation of RBD and SRBD were shown in black and blue curves between 20 °C to 95 °C monitored at 222 nm.

(d) Flow chart of NAb analysis in mouse sera and ELISA of RBD NAb at days 42. (n = 5 mice in each group).

(e) H&E staining of major organs in AAV-CAG-GFP and AAV-CAG-SRBD mice. Values are means  $\pm$  SEM. Scale bar: 100  $\mu$ m.

Fig. 2

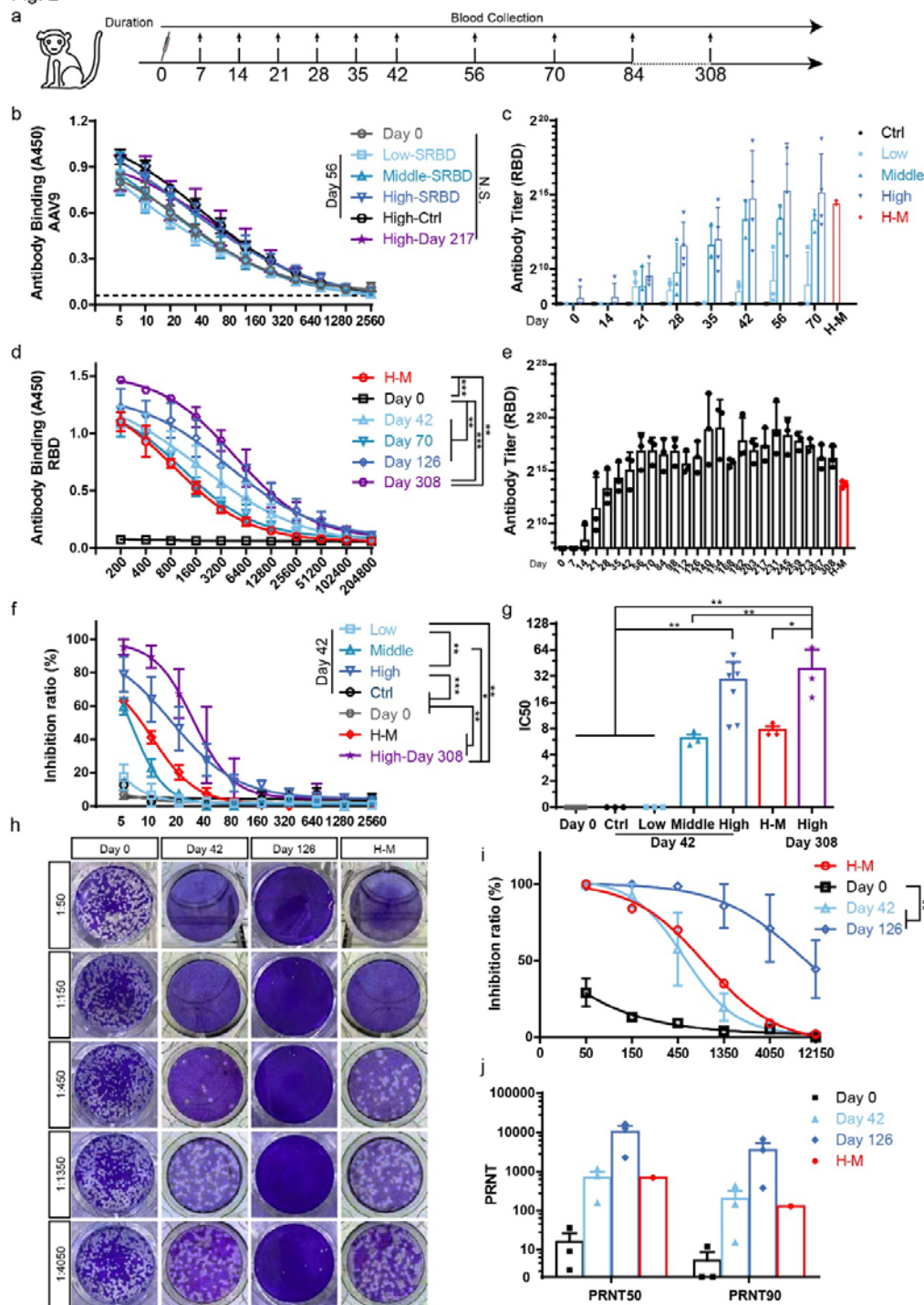


**Figure 2. Single-dose SRBD vaccine elicits a long-term and high NAb response in rhesus macaques.**

(a) Experimental strategy of immunization and blood test for AAV-SRBD vaccine in

rhesus macaques.

(b) ELISA of NABs in the sera of macaques against AAV2/9. (Day 0: sera collected before intramuscular injection; Low/Middle/High-SRBD: 56 days post injection of low/middle/high-dose SRBD vaccine; High-Ctrl: 56 days post injection of high-dose AAV-CAG-GFP control; High-Day 217: 217 days post injection of high-dose SRBD vaccine; n = 3 macaques in Low-SRBD, Middle-SRBD, High-Ctrl, High-Day 217 groups; n = 7 macaques in Day 0 group; n = 4 macaques in High-SRBD group).

(c) NAb analysis of RBD from days 0 to 70 in the macaque sera of low/middle/high-dose groups and AAV-CAG-GFP control (n = 3 macaques in Ctrl, Low and Middle group ; n = 3 repeats in H-M group; n = 4 macaques in High group).

(d) ELISA of RBD NABs at days 42, 70, 126, and 308. (H-M: mixed sera of convalescent patients; D0: sera collected before intramuscular injection; Day 42/70/126/308: sera collected on 42/70/126/308 days post injection of high-dose SRBD vaccine; n = 3 repeats in H-M group; n = 3 macaques in other groups).

(e) ELISA of RBD NABs from days 0 to 308 after high-dose vaccine (n = 3 repeats in H-M group; n = 3 macaques in other groups).

(f) Competitive ELISA of RBD NABs to inhibit interactions between ACE2 and RBD. (Day 0: sera collected before intramuscular injection; Low/Middle/High: 42 days post injection of low/middle/high-dose SRBD vaccine; Ctrl: 42 days post injection of high-dose AAV-CAG-GFP control, H-M: mixed sera from convalescent patients; High-Day 308: 308 days post injection of high-dose SRBD vaccine; n = 3 macaques in Ctrl, Low, Middle group and High Day 308 groups; n = 3 repeats in H-M group; n = 7 macaques in High group; n = 16 macaques in Day 0 group).

(g) Half maximal inhibitory concentrations (IC<sub>50</sub>) of NABs against RBD calculated by competitive ELISA.

(h) Representative images of NAb test in Vero E6 cells.

(i) Inhibition curve of NAb test (n = 3 macaques in Day 0, Day 42, and Day 126 groups; n = 1 in H-M group).

(j) PRNT50 and PRNT90 calculated by NAb test.

Values are means  $\pm$  SEM or geometric mean + geometric standard deviation for antibody titer.



Fig. 3

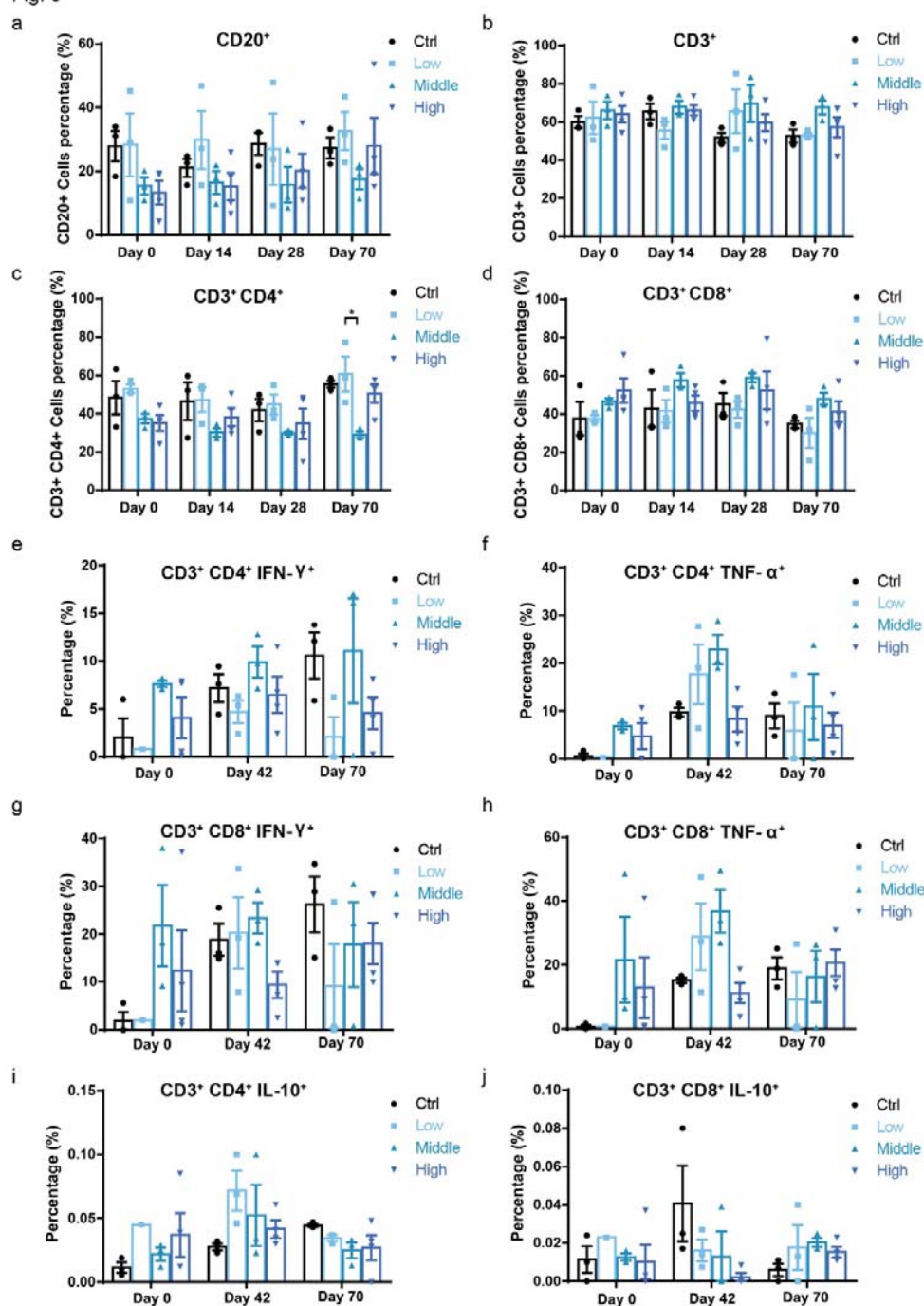


**Figure 3. Safety evaluation of SRBD vaccine in rhesus macaques.**

(a) Percentage of CD20-positive cells in the sera of high/middle/low-dose and control rhesus macaques (Ctrl: intramuscular injection with high-dose AAV-CAG-GFP)



control; Low/Middle/High: intramuscular injection of low/middle/high-dose SRBD vaccine).

(b) Percentage of CD3-positive cells in the sera of high/middle/low-dose and control rhesus macaques.

(c) Percentage of CD3- and CD4-positive cells in the sera of high/middle/low-dose and control rhesus macaques.

(d) Percentage of CD3 and CD8-positive cells in the sera of high/middle/low-dose and control rhesus macaques

(e) Percentage of CD3-, CD4-, and IFN- $\gamma$ -positive cells in the sera of high/middle/low-dose and control rhesus macaques

(f) Percentage of CD3-, CD4-, and TNF- $\alpha$ -positive cells in the sera of high/middle/low-dose and control rhesus macaques.

(g) Percentage of CD3-, CD8-, and IFN- $\gamma$ -positive cells in the sera of high/middle/low-dose and control rhesus macaques.

(h) Percentage of CD3-, CD8-, and TNF- $\alpha$ -positive cells in the sera of high/middle/low-dose and control rhesus macaques.

(i) Percentage of CD3-, CD4-, and IL-10-positive cells in the sera of high/middle/low-dose and control rhesus macaques.

(j) Percentage of CD3-, CD8-, and IL-10-positive cells in the sera of high/middle/low-dose and control rhesus macaques.

(n = 3 macaques in Ctrl, Low, and Middle groups; n = 4 macaques in High group).

Fig. 4

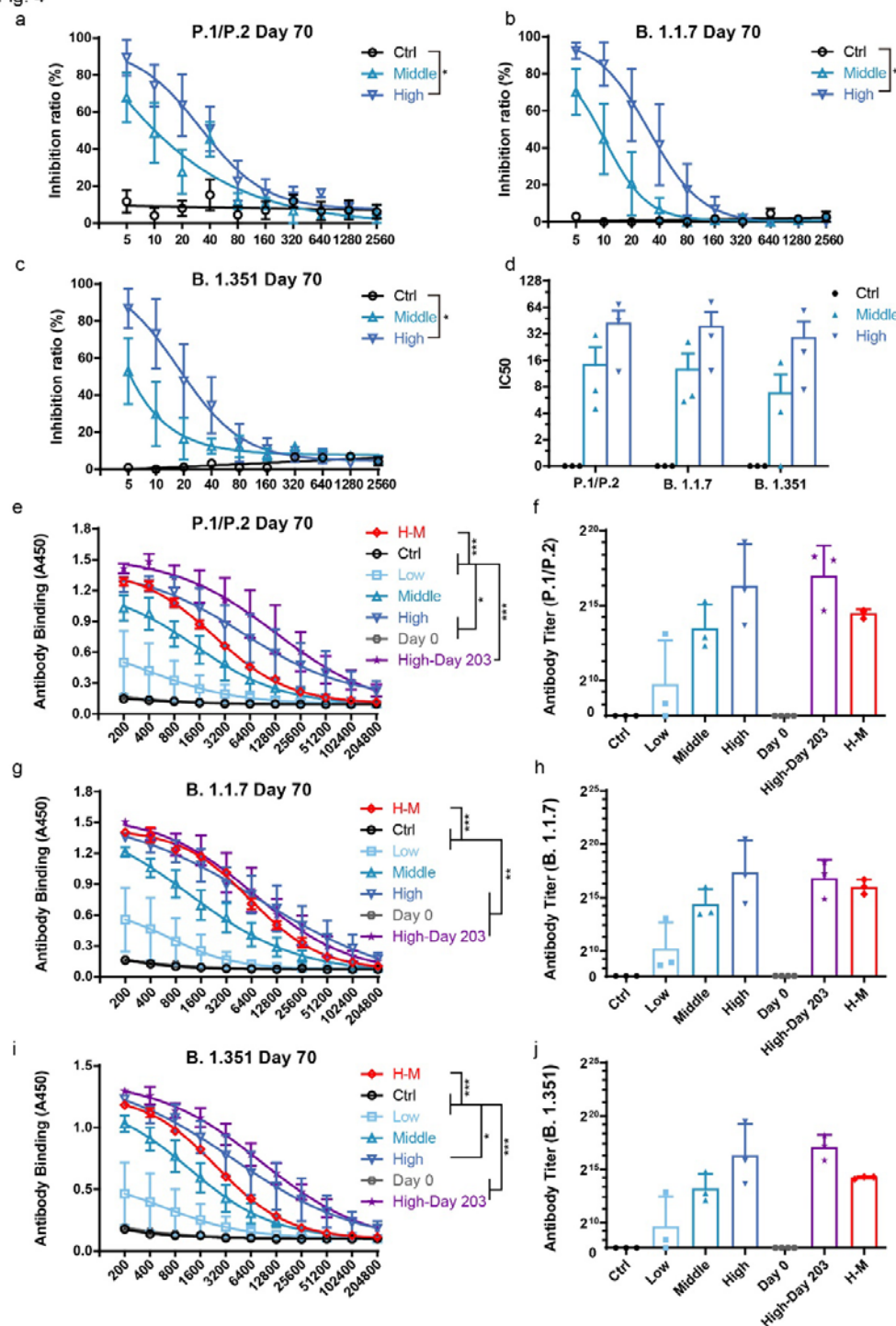


**Figure 4. SRBD vaccine immunization elicits a long-term and high NAb response in rhesus macaques against SARS-CoV-2 variants.**

(a) Competitive ELISA on inhibition of interactions between ACE2 and SARS-CoV-2

variants P.1/P.2 RBD by NAbs. (Middle/High: 70 days post injection of middle/high-dose SRBD vaccine; Ctrl: 70 days post injection of high-dose AAV-CAG-GFP control; n = 3 macaques in each group).

(b) Competitive ELISA on inhibition of interactions between ACE2 and SARS-CoV-2 variants B.1.1.7 RBD by NAbs (n = 3 macaques in each group).

(c) Competitive ELISA on inhibition of interactions between ACE2 and SARS-CoV-2 variant B.1.351 RBD by NAbs (n = 3 macaques in each group).

(d) IC<sub>50</sub> values of NAbs in (a-c) calculated by competitive ELISA (n = 3 macaques in each group).

(e) ELISA of NAbs against SARS-CoV-2 variants P.1/P.2 RBD. (H-M: mixed sera of convalescent patients; Day 0: sera collected before intramuscular injection; Low/Middle/High: 70 days after intramuscular injection of low/middle/high-dose SRBD vaccine; Ctrl: 70 days after intramuscular injection of high-dose of AAV-CAG-GFP control; High-Day 203: 203 days after intramuscular injection of high-dose SRBD vaccine; n = 4 macaques in Day 0 group; n = 3 repeats in H-M group; n = 3 macaques in other groups).

(f) Antibody titer calculated by ELISA against SARS-CoV-2 variants P.1/P.2 RBD (n = 4 macaques in Day 0 group; n = 3 repeats in H-M group; n = 3 macaques in other groups).

(g) ELISA of NAbs against SARS-CoV-2 variant B.1.1.7 RBD (n = 4 macaques in Day 0 group; n = 3 repeats in H-M group; n = 3 macaques in other groups).

(h) Antibody titer calculated by ELISA of NAbs against SARS-CoV-2 variant B.1.1.7 RBD (n = 4 macaques in Day 0 group; n = 3 repeats in H-M group; n = 3 macaques in other groups).

(i) ELISA of NAbs against SARS-CoV-2 variant B.1.351 RBD (n = 4 macaques in

Day 0 group; n = 3 repeats in H-M group; n = 3 macaques in other groups).

(j) Antibody titer calculated by ELISA of NAbs against SARS-CoV-2 variant B.1.351 RBD (n = 4 macaques in Day 0 group; n = 3 repeats in H-M group; n = 3 macaques in other groups).

Values are means  $\pm$  SEM or geometric mean + geometric standard deviation for antibody titer.

Fig. S1

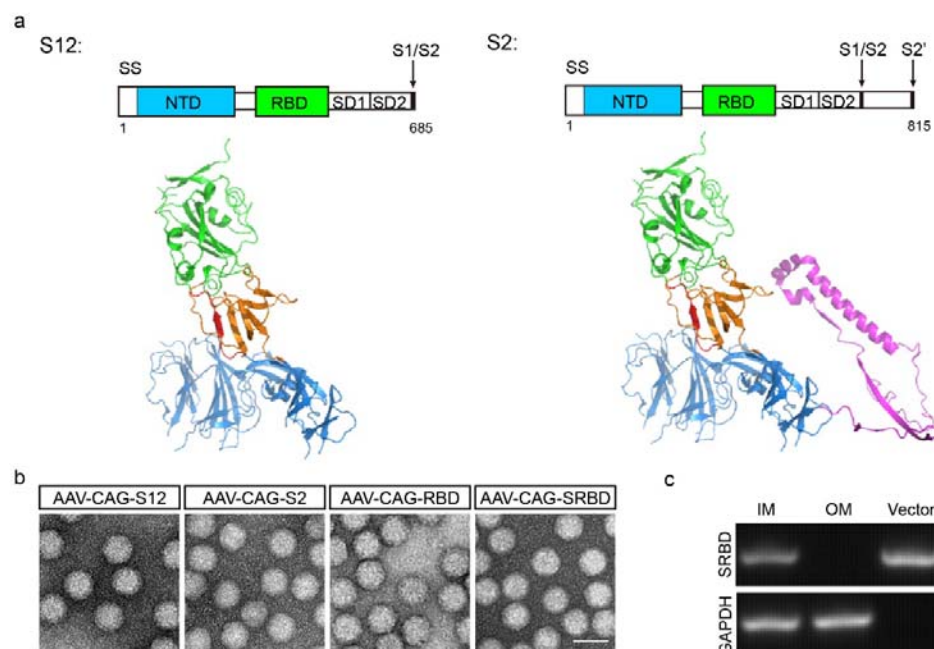


**Figure S1. AAV-delivered vaccine for COVID-19.**

(a) Structural analysis of S1 and S12.

(b) Electron microscopic images of AAV-delivered vaccines.

(c) mRNA expression of SRBD in SRBD-vaccinated mice.

Scale bar: 50 nm.

Fig. S2

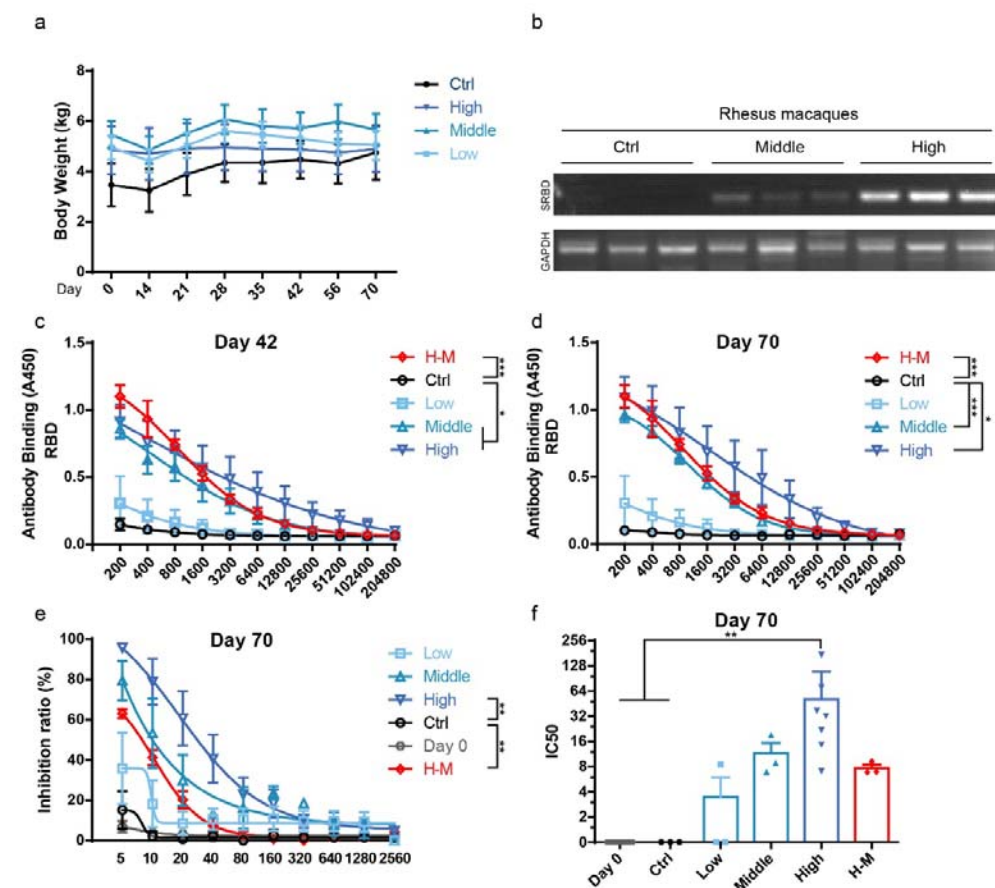


**Figure S2. Single-dose SRBD vaccine immunization in rhesus macaques.**

(a) No body weight changed from days 0 to 70 in different dose groups. (Ctrl: macaques intramuscularly injected with high-dose of AAV-CAG-GFP control; Low/Middle/High: macaques intramuscularly injected with low/middle/high-dose of SRBD vaccine; n = 3 macaques in Ctrl, Low, and Middle groups; n = 4 macaques in High group).

(b) RT-PCR of SRBD and GAPDH in muscle cells injected with different doses of SRBD vaccine.

(c) ELISA of NAb against RBD on day 42 with low/middle/high-dose SRBD vaccine or high-dose AAV-CAG-GFP control (n = 3 macaques in Ctrl, Low and Middle group ;

n = 3 repeats in H-M group; n = 4 macaques in High group).

(d) ELISA of NAbs at day 70 with low/middle/high-dose SRBD vaccine or high-dose AAV-CAG-GFP control (n = 3 macaques in Ctrl, Low and Middle group ; n = 3 repeats in H-M group; n = 4 macaques in High group).

(e) Competitive ELISA on inhibition of interactions between ACE2 and RBD by NAbs at day 70 (n = 3 macaques in Ctrl, Low and Middle group ;n = 3 repeats in H-M group; n = 4 macaques in High group; n = 16 macaques in Day 0 group).

(f) IC<sub>50</sub> values of NAbs on day 70 calculated by competitive ELISA.

Values are means  $\pm$  SEM

Fig. S3

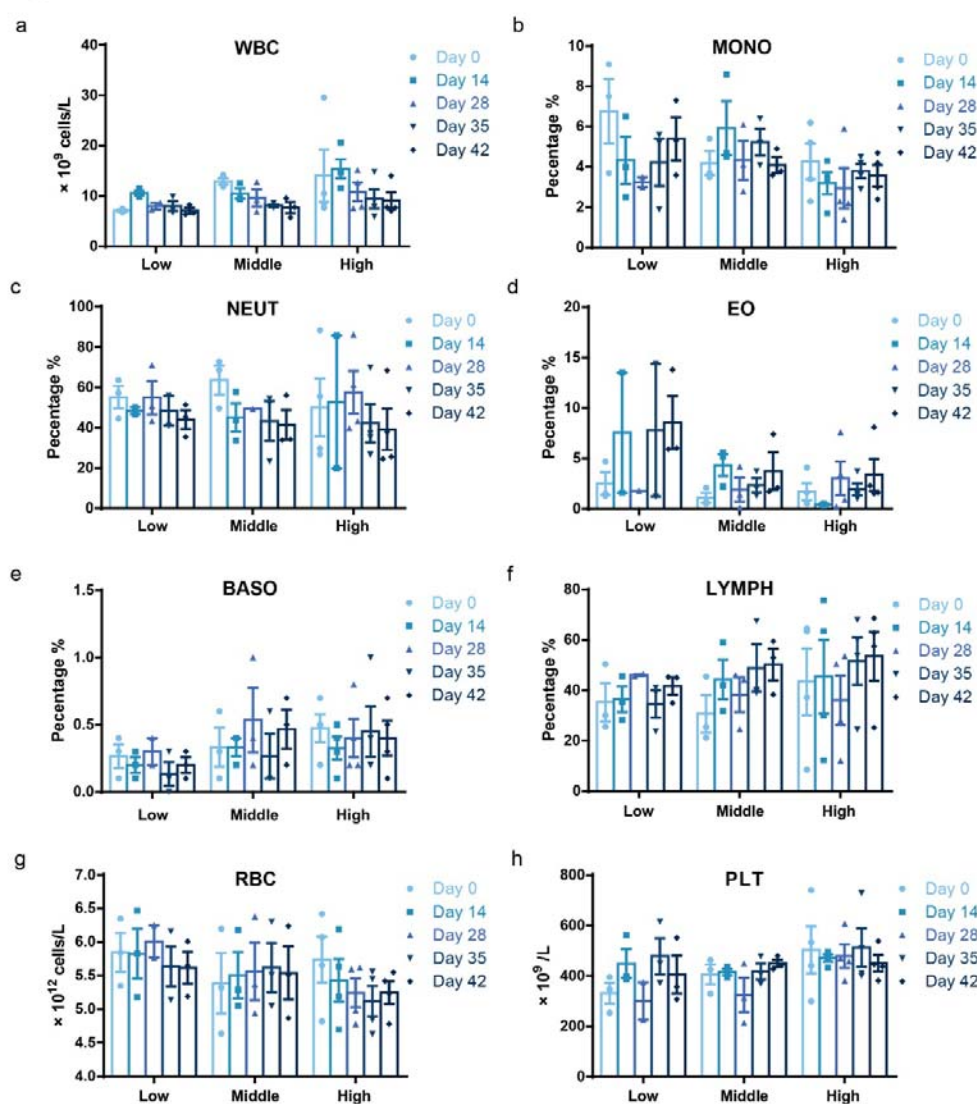


**Figure S3. Pathological indicators in blood of macaques following intramuscular injection of AAV-SRBD vaccine.**

(a) White blood cell (WBC) count in the sera of high/middle/low-dose rhesus macaques.

(b) Monocyte cell (MONO) percentage in the sera of high/middle/low-dose rhesus macaques.

(c) Neutrophil cell (NEUT) percentage in the sera of high/middle/low-dose rhesus



macaques.

(d) Eosinophil cell (EO) percentage in the sera of high/middle/low-dose rhesus macaques.

(e) Basophil cell (BASO) percentage in the sera of high/middle/low-dose rhesus macaques.

(f) Lymphocyte cell (LYMPH) percentage in the sera of high/middle/low-dose rhesus macaques.

(g) Red blood cell (RBC) count in the sera of high/middle/low-dose rhesus macaques.

(h) Platelet (PLT) count in the sera of high/middle/low-dose rhesus macaques.

(n = 3 macaques in Low and Middle groups; n = 4 macaques in High group).

Values are means  $\pm$  SEM

Fig. S4

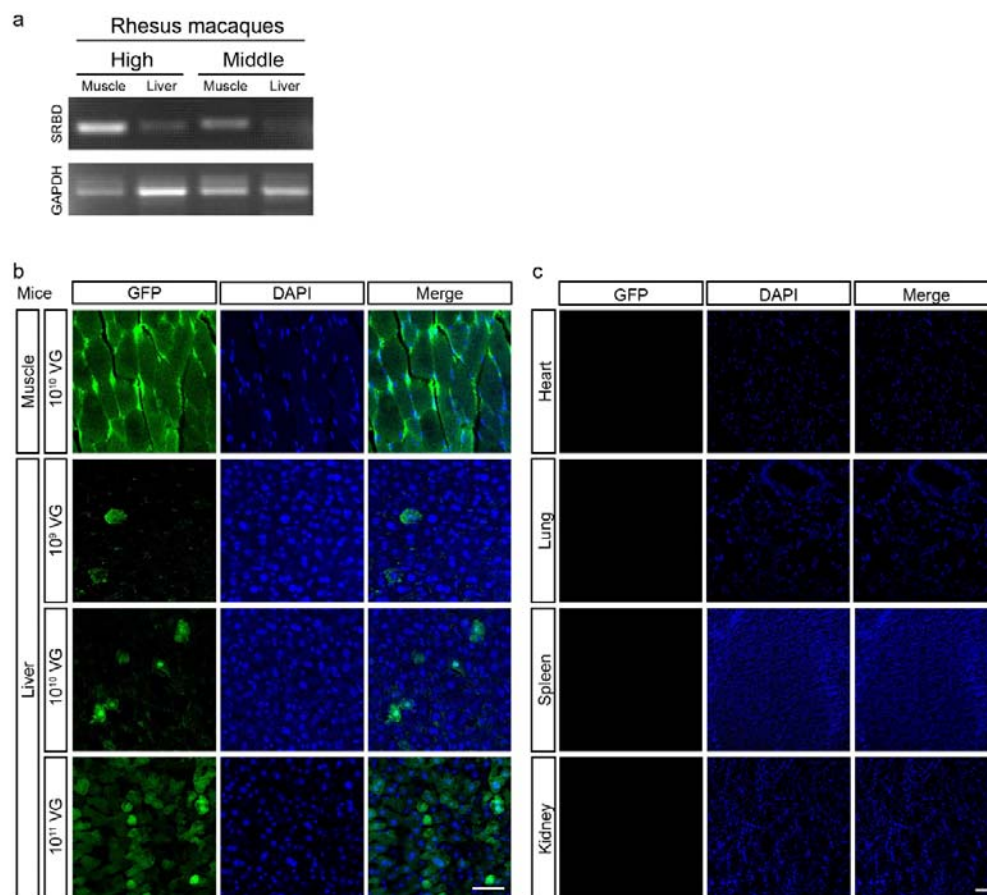


**Figure S4. The infection of AAV in the muscles and liver of macaques, and the major organs of mice.**

(a) RT-PCR of SRBD in muscle and liver cells from high- and middle-dose macaques.

(b) Immunohistochemistry analysis of mouse muscle and liver cells in low/middle/high-dose AAV-CAG-GFP mice.

(c) Immunohistochemistry analysis of major tissues (i.e. heart, lung, spleen and kidney) in mice following intramuscular injection with high-dose AAV-CAG-GFP.

Scale bar: 50  $\mu$ m

Fig. S5

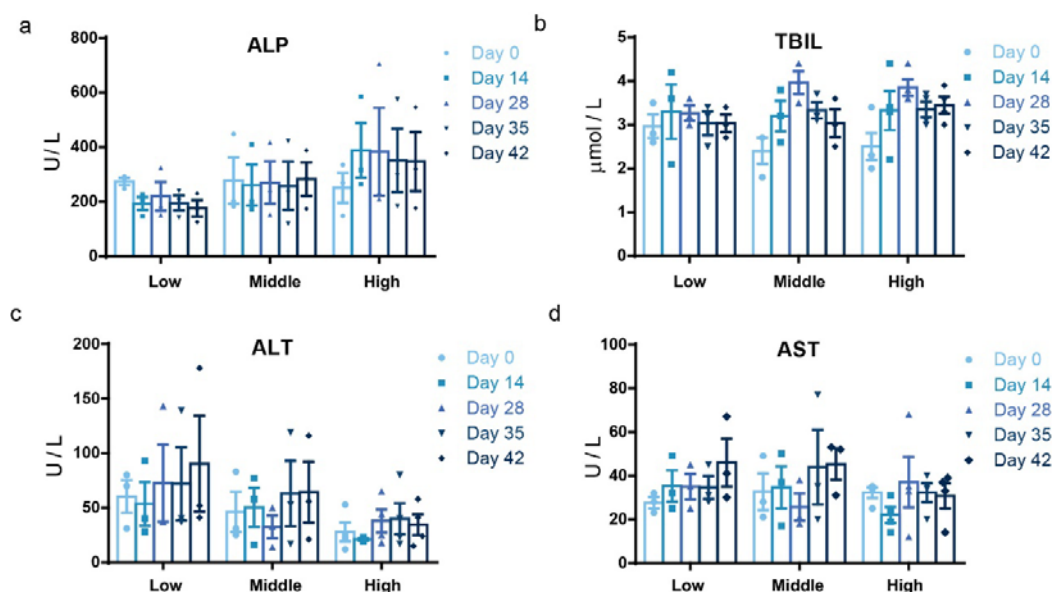


**Figure S5. Pathological indicators in liver of macaques following AAV-SRBD intramuscular injection.**

(a) Alkaline phosphatase (ALP) level in the sera of high/middle/low-dose rhesus macaques.

(b) Total bilirubin (TBIL) level in the sera of high/middle/low-dose rhesus macaques.

(c) Alanine aminotransferase (ALT) level in the sera of high/middle/low-dose rhesus macaques.

(d) Aspartate aminotransferase (AST) level in the sera of high/middle/low-dose rhesus macaques.

(n = 3 macaques in Low and Middle groups; n = 4 macaques in High group).

Values are means  $\pm$  SEM

Fig. S6

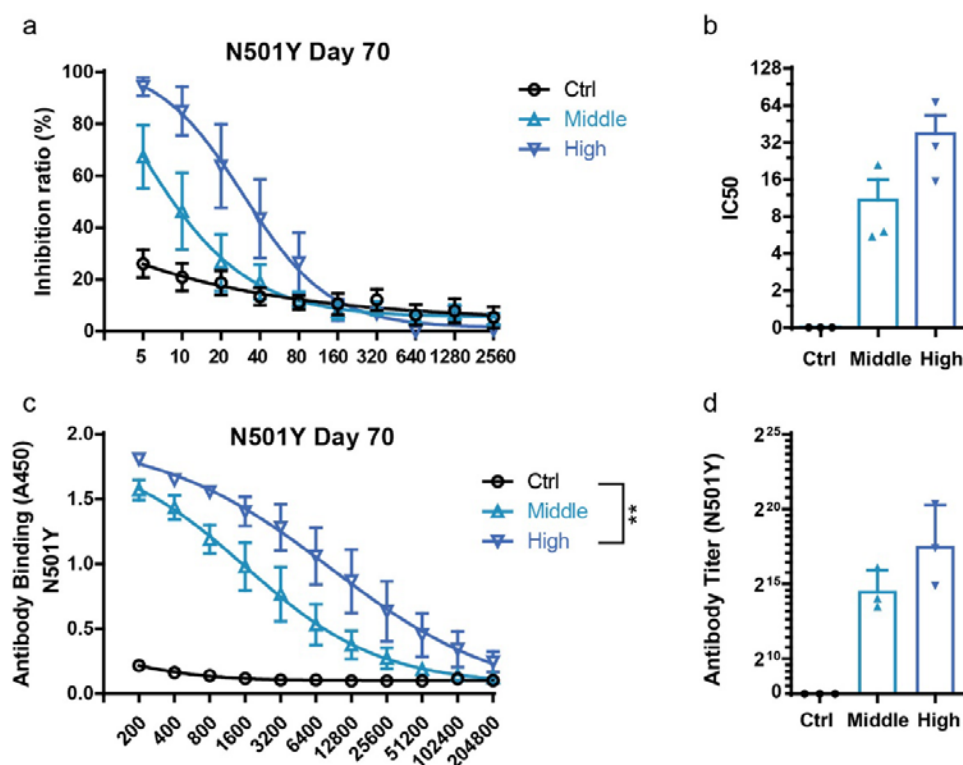


**Figure S6. Immunization of AAV-SRBD vaccine elicits a long-term and high NAbs response in rhesus macaques against RBD N501Y.**

(a) Competitive ELISA on inhibition of interactions between ACE2 and RBD N501Y by NAbs (n = 3 macaques in each group).

(b) IC<sub>50</sub> values of NAbs in (a) calculated by competitive ELISA.

(c) ELISA of NAbs against RBD N501Y (n = 3 macaques in each group).

(d) Antibody titers calculated by ELISA of NAbs against RBD N501Y.

Values are means  $\pm$  SEM or geometric mean + geometric standard deviation for antibody titer.